Rev. Roum. Sci. Techn.– Électrotechn. et Énerg.
Vol. **68**, *1*, pp. 18–23, Bucarest, 2023

PROPORTIONAL INTEGRAL QUASI-RESONANT CONTROLLER FOR ZERO-SEQUENCE CIRCULATING CURRENT AND RIPPLE SUPPRESSION IN PARALLEL THREE-PHASE RECTIFIERS

ALI CHEBABHI[1], AL-DWA ALA ADDIN MOHAMMED HUSIN[1], SAID BARKAT[1], MOHAMMED KARIM FELLAH[2]

Keywords: Parallel three-phase pulse with modulation rectifiers; Zero-sequence circulating current; Harmonics; Proportional integral quasi-resonant controller.

Parallel three-phase pulse width modulation (PWM) rectifiers with standard dc and ac buses are widely used in power systems due to their many advantages: flexibility, sinusoidal grid currents, lower switching frequency, and good reliability. However, this topology suffers from zero-sequence circulating current (ZSCC) generated by numerous reasons, including unbalanced filter inductors, unequal dead time, and losses of synchronism between the control of each rectifier will distort the ac-side currents and increase power losses. This paper proposes an adjusted space vector pulse width modulated (ASVPWM) method and a proportional integral quasi-resonant controller (PIQRC) method to force the ZSCC to be zero and to reduce its ripples, which results in low-frequency harmonic components in the ac side currents. This twofold objective can be achieved by adjusting the zero-vector duty ratios of ASVPWM to suppress the ZSCC and by using PIQRC to mitigate its predominant harmonics. Finally, the superiority and efficiency of the proposed control method in terms of ZSCC suppression and current ripple reduction are verified through comparative analysis with the conventional ZSCC-PI controller.

1. INTRODUCTION

Parallel three-phase PWM rectifiers are widely used in high power conversion, high voltage direct current systems, and renewable energy applications such as wind turbine generation [1,2]. This configuration offers an interesting alternative for increasing the system capacity, reducing the switching constraints with transmission efficiency and fractionation of the high ac grid currants, and enhancing the grid's stability and reliability [3].

However, a zero-sequence circulating current (ZSCC) flow path is formed in all parallel PWM converters configurations. The ZSCC between these paralleled converters is produced by the differences in filter inductors, unequal current measurements, and dead times [4,5]. Unfortunately, the ZSCC results in low-frequency harmonic components in the ac side currents, especially the third harmonic and its multiples, which increases the distortion and switching losses, reduces the efficiency and degrades the overall performance of the parallel systems [6–9].

Various control strategies are proposed to suppress the ZSCC in parallel PWM converters to address this problem. High-frequency harmonic components of ZSCC are accurately reduced to a suitable level by an appropriate choice of filter inductors [10]. Discontinuous PWM control minimizing the ZSCC was proposed in [11,12]. Reducing ZSCC is the advantage of this strategy but it causes a high ripple in the output currents.

The selection of design parameters (SDP) control strategy to reduce the ZSCC was proposed for parallel shunt active filters (SAFs) in [13]. An enhanced SDP control strategy was used to control the parallel SAFs. However, due to the nature of ZSCC, more than this method is needed to give good performance.

A carrier phase shift PWM control strategy was proposed in [14] for suppressing the ZSCC for modular interleaved converters. This strategy has good steady-state performance and fast dynamic response but suffers from high switching losses in high power applications. For this, applying SVPWM strategies in high power applications is more suitable since they can significantly reduce the switching losses [15–19]. In [16,17], adjustable duty ratios based on PI controller was proposed to suppress the ZSCC in the paralleled inverters. A zero-vector feedforward with PI control to suppress the ZSCC was proposed in [18,19]. These strategies are effective in suppressing the ZSCC but not enough in enhancing the power quality due to high ZSCC ripples.

The suppression above methods focused much more on the reduction of ZSCC not on its cancellation, which impacts the power quality of the grid side currents. In this paper, the ZSCC as well as the third harmonic and its multiples in the ac side currents, will be suppressed by controlling the ZSCC by using the proposed PIQRC. The proposed control can suppress the ZSCC and the 3rd and 9th harmonics in the two parallel PWM rectifier input currents by adjusting the duty ratio of zero states of one of the two SVPWM. For this, the state vector duty ratios of ASVPWM are parameterized by a control variable generated by the proposed PIQR controller.

In addition, the use of PIQRC instead of the PI controller allows the suppression of low-frequency harmonics of the ZSCC. Also, the proposed PIQRC approach can be optionally designed only for specific harmonics, which provide high robustness, efficiency, and flexibility. It can achieve zero-steady-state error at the harmonics that need to be eliminated with rather fast dynamics. On the other hand, the PIQRC has very small effect on the parameter determination of the ZSCC control loop, which facilitates the elimination of harmonics and the control design.

The rest of the paper is arranged as follows: section 2 presents the modeling of the parallel PWM rectifiers. Modeling and analysis of the ZSCC is detailed in section 3. Control of ZSCC using proposed ASVPWM method with ZSCC-PIQR controller is detailed in section 4. Simulation results are illustrated and discussion in Section V. Finally, a conclusion is drawn in Section VI.

2. SYSTEM MODELING

The adopted power circuit of two parallel PWM rectifiers with common dc bus is illustrated in Fig. 1.

[1] EE Laboratory, University of Msila, Algeria. ali.chebabha@univ-msila.dz; aldawah.alaa@univ-msila.dz; said.barkat@univ-msila.dz
[2] ICEPS Laboratory, Djillali Liabes University of Sidi Bel-Abbes, Algeria. mkfellah@gmail.com

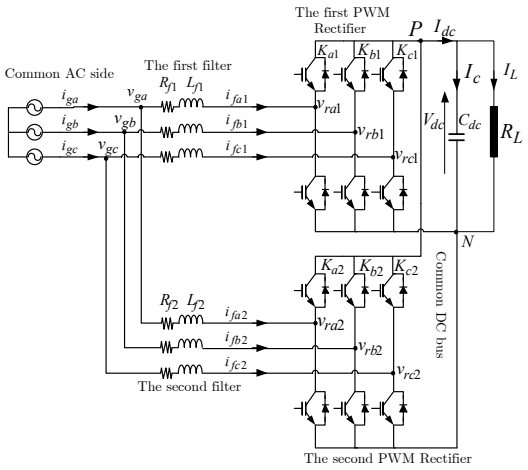

Fig. 1 – Power circuit of two paralleled three-phase PWM rectifiers.

The dynamic equations describing the ac and dc sides' currents of the two PWM rectifiers shown in Fig. 1 can be defined in the synchronous rotating frame (dq) by [10] as:

$$\begin{cases} L_{f1}\dfrac{\mathrm{d}i_{fd1}}{\mathrm{d}t}=-R_{f1}i_{fd1}+v_{gd}-d_{d1}V_{dc}-\omega L_{f1}i_{fq1} \\ L_{f1}\dfrac{\mathrm{d}i_{fq1}}{\mathrm{d}t}=-R_{f1}i_{fq1}+v_{gq}-d_{q1}V_{dc}+\omega L_{f1}i_{fd1} \\ L_{f2}\dfrac{\mathrm{d}i_{fd2}}{\mathrm{d}t}=-R_{f2}i_{fd2}+v_{gd}-d_{d2}V_{dc}-\omega L_{f2}i_{fq2} \\ L_{f2}\dfrac{\mathrm{d}i_{fq2}}{\mathrm{d}t}=-R_{f2}i_{fq2}+v_{gq}-d_{q2}V_{dc}+\omega L_{f2}i_{fd2} \\ C_{dc}\dfrac{\mathrm{d}V_{dc}}{\mathrm{d}t}=d_{dx}i_{fdx}+d_{qx}i_{fqx} \end{cases}, \quad (1)$$

where i_{fdx} and i_{fqx} are the dq-axes input currents of rectifier x (x=1,2), respectively, ω is the grid angular frequency, and $v_{rdx}=d_{dx}i_{fdx}$ and $v_{rqx}=d_{qx}i_{fqx}$ are the rectifier x d-axis and q-axis input voltages, respectively. d_{dx} and d_{qx} are the duty ratio of rectifier x in the dq-frame.

3. MODELING AND ANALYSIS OF ZSCC IN PARALLELED PWM RECTIFIERS

The ZSCC is caused essentially by the differences in filters inductors, which can be defined as: [15]:

$$i_{zx}=\frac{i_{fax}+i_{fbx}+i_{fcx}}{3}, \quad (2)$$

where $i_{z2}=-i_{z1}$.

The equivalent model of ZSCC for the two rectifiers can be derived from eq. (1) and eq. (2) as follows [15]:

$$\begin{cases} L_{f1}\dfrac{\mathrm{d}i_{z1}}{\mathrm{d}t}=-R_{f1}i_{z1}+d_{z1}V_{dc}=0 \\ L_{f2}\dfrac{\mathrm{d}i_{z2}}{\mathrm{d}t}=-R_{f2}i_{z2}+d_{z2}V_{dc}=0 \end{cases}, \quad (3)$$

where d_{z1} and d_{z2} are the zero-sequence duty ratios (ZSDRs) of rectifiers 1 and 2, respectively, which can be given as:

$$d_{zx}=d_{ax}+d_{bx}+d_{cx}, \quad (4)$$

By subtracting the two equations in eq. (3), the average model of ZSCC system can be obtained as:

$$(L_{f1}+L_{f2})\frac{\mathrm{d}i_{z2}}{\mathrm{d}t}+(R_{f1}+R_{f2})i_{z2}=(d_{z2}-d_{z1})V_{dc}, \quad (5)$$

where $\Delta d_z=d_{z2}-d_{z1}$ is the difference of ZSDRs. The ZSCC equivalent circuit is shown in Fig. 2, while $v_{zx}=d_{zx}V_{dc}$ is the zero-sequence voltage (ZSV) of each PWM rectifier.

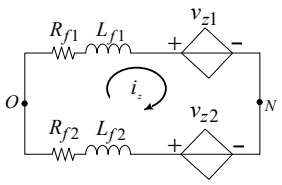

Fig. 2 – ZSCC equivalent circuit for paralleled two rectifiers.

The equivalent circuit in Fig. 2 and eq. (5) indicates that the difference between the ZSDRs is the essential factor to generate the ZSCC, which could be the result generally of mismatches in the filters inductances. If the ZSDRs d_{z1} and d_{z2} are the same, ZSCC will not be generated. These ZSDRs have a periodic triangular waveform of frequency equal to 150 Hz (triple of grid voltage frequency) and have equal magnitude but with a phase difference [15, 16]. Note also that the difference between the ZSDRs is a periodic square wave with a triple grid voltage frequency. So, the ZSCC can be successfully suppressed when the difference between the ZSDRs is set to zero.

4. CONTROL STRATEGY BASED ON ADJUSTING SPACE VECTOR PULSE WIDTH MODULATED

The voltage-oriented control (VOC) with the proposed ASVPWM method of the parallel two PWM rectifiers is shown in Fig. 3 [20,21].

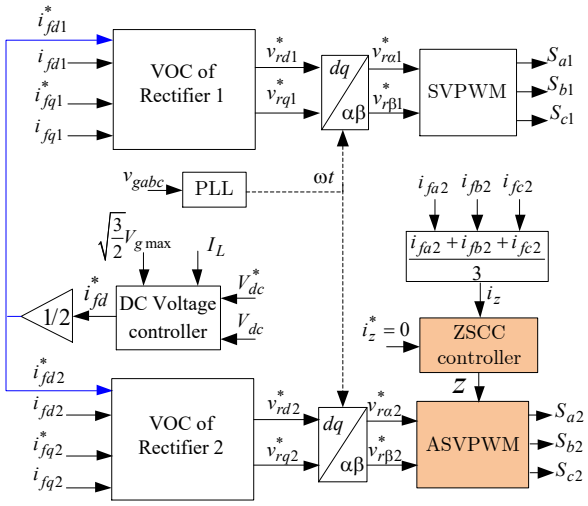

Fig. 3 – Control scheme of paralleled two three-phase PWM rectifiers.

When the system operates in unity power factor, the reference i_{fq}^* is set to zero and the reference i_{fd}^* is determined by the DC-bus voltage controller [22].

4.1. CONVENTIONNEL SPACE VECTOR PULSE WIDTH MODULATION

In each switching period T_s, the reference voltage of each SVPWM can be synthesized by two adjacent nonzero state vectors and two zero state vectors as shown in Fig. 4(a) [23]. This figure represents the distribution of the two adjacent nonzero state vectors and the two zero state vectors in sector I of αβ frame.

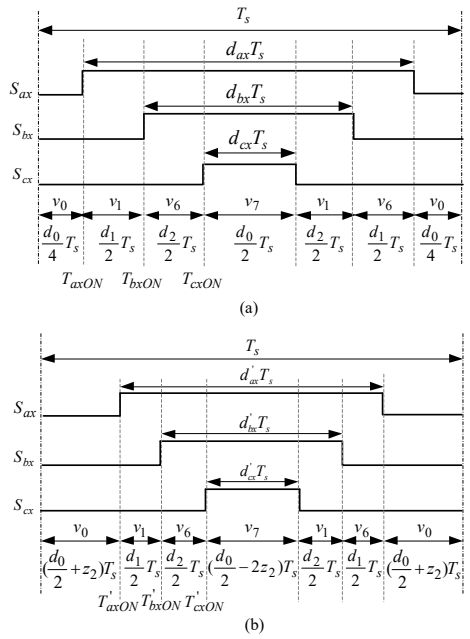

Fig. 4 – State vectors and their duty rations in sector I: a) conventional SVPWM, b) adjusted SVPWM.

As shown in Fig. 4(a), the ZSDR d_{zx} of rectifier x in eq. (4) is linked to the duty ratios of state vectors by:

$$d_{zx} = \left(d_{1x} + d_{2x} + \frac{d_{0x}}{2}\right) + \left(d_{2x} + \frac{d_{0x}}{2}\right) + \frac{d_{0x}}{2}, \quad d_{zx} = d_{1x}+2d_{2x}+\frac{3d_{0x}}{2} \tag{6}$$

where d_{1x} and d_{2x} are the two nonzero vectors duty ratios of rectifier x.

As shown in Fig. 4(a), zero vectors duty ratio d_{0x} can be expressed as:

$$d_{0x} = 1-d_{1x}-d_{2x}, \tag{7}$$

The switching times T_{axON}, T_{bxON}, and T_{cxON} of the state vectors are expressed as:

$$\begin{cases} T_{axON}=\frac{d_{0x}}{2}T_s \\ T_{bxON}=T_{axON}+\frac{d_{1x}}{2}T_s \\ T_{cxON}=T_{bxON}+\frac{d_{2x}}{2}T_s \end{cases}, \tag{8}$$

4.2. PROPOSED ADJUSTED SPACE VECTOR PULSE WIDTH MODULATION

In order to eliminate the ZSCC, a modified version of the previous SVPWM is proposed in which a variable z is introduced in order to suppress the difference between the ZSDRs. This variable z can be introduced into d_{0x} for adjusting the time application of the zero vectors in each switching period as shown in Fig. 4(b). Thus, d_{0x} is changed to $\left(\frac{d_{0x}}{2}-z_x\right)T_s$ and $\left(\frac{d_{0x}}{2}+z_x\right)T_s$, respectively [15]. The ZSDR d'_{zx} after adjusting the variable z are expressed as:

$$\begin{aligned} d'_{zx} &= d'_{ax} + d'_{bx} + d'_{cx} \\ &= \left(d_{1x}+d_{2x}+\frac{d_{0x}}{2}-2z_x\right)+\left(d_{2x}+\frac{d_{0x}}{2}-2z_x\right)+\left(\frac{d_{0x}}{2}-2z_x\right), \\ d'_{zx} &= d_{1x}+2d_{2x}+\frac{3d_{0x}}{2}-6z_x \end{aligned} \tag{9}$$

The distribution of state vectors and their duty rations in the sector I of ASVPWM is shown in Fig. 4(b).

The average model in eq. (5) after adjustment becomes:

$$\left(L_{f1}+L_{f2}\right)\frac{\mathrm{d}i_{z2}}{\mathrm{d}t}+\left(R_{f1}+R_{f2}\right)i_{z2}=\left(d'_{z2}-d'_{z1}\right)V_{dc}, \tag{10}$$

The difference between the new ZSDRs $\Delta d_z=d'_{z2}-d'_{z1}$ between PWM rectifiers 1 and 2 is calculated as:

$$\Delta d_z=\left(d_{12}+2d_{22}+\frac{3d_{02}}{2}-6z_2\right)-\left(d_{11}+2d_{21}+\frac{3d_{01}}{2}-6z_1\right), \tag{11}$$

In the two parallel PWM rectifiers, the control of ZSCC is chosen to be done by adjusting the variable z_2 while the variable z_1 is set to zero (rectifier 1 is controlled by the conventional SVPWM).

In the ASVPWM, the new switching times T'_{axON}, T'_{bxON}, and T'_{cxON} after adjustment are expressed as:

$$\begin{cases} T'_{axON}=T_{axON}+z_2T_s \\ T'_{bxON}=T'_{axON}+\frac{d_{1x}}{2}T_s \\ T'_{cxON}=T'_{bxON}+\frac{d_{2x}}{2}T_s \end{cases}, \tag{12}$$

Substituting eqs. (7) and (11) or eqs. (7), (8), and (12) into eq. (10), eq. (10) results in:

$$\left(L_{f1}+L_{f2}\right)\frac{\mathrm{d}i_{z2}}{\mathrm{d}t}=-\left(R_{f1}+R_{f2}\right)i_{z2}+\frac{1}{2}\left(\Delta D_{12}-12z_2\right)V_{dc}, \tag{13}$$

where $\Delta D_{12}=d_{12}+2d_{22}-d_{11}-2d_{21}$

By neglecting the effects of ΔD_{12} and by applying the Laplace Transform on eq. (13), the ZSCC in Laplace domain can be expressed as:

$$I_{z2}(s)=\frac{6Z_2(s)V_{dc}}{\left(L_{f1}+L_{f2}\right)s+\left(R_{f1}+R_{f2}\right)}, \tag{14}$$

where $Z_2(s)$ is the Laplace transform of z_2.

4.3. PROPOSED PI QUASI-RESONANT CONTROL

As described above, the ZSCC generated by difference between the ZSDRs under unbalanced filters inductors has a triangular periodic waveform with the characteristic of triple grid voltage frequency (150 Hz), making it mainly composed of the third harmonic component and its triple multiples. Thus, the PI controller is unable to accurately compensate for the variable z_2 with periodic waveforms of 150 Hz due to its lower bandwidth [16].

In this section, a PIQRC will be proposed for controlling the ZSCC by providing an accurate z_2 with a periodic waveform of 150 Hz, thereby effectively suppressing the 3rd harmonic and its triple multiples of ZSCC and their impacts on the input currents. The schematic diagram of the proposed PIQRC is shown in Fig. 5.

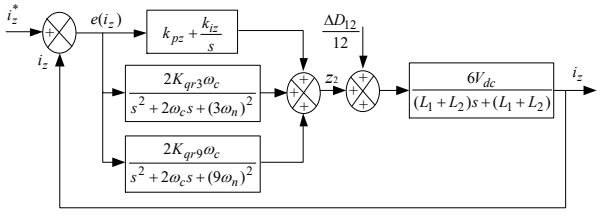

Fig. 5 – Proposed PIQRC of zero-sequence circulating current control.

The goal of this proposed controller is to provide the variable z_2, which will be added to the duty ratios of zero vectors in order to accurately suppress the difference

between the ZSDRs, as well as suppress the ZSCC and eliminate the lower harmonics in the input currents of the two PWM rectifiers [23, 24]. In the following, the PIQRC is designed to suppress the 3rd and 9th harmonics in the input currents of the two PWM rectifiers. Thus, the variable z_2 is given by:

$$z_2 = e_{\dot{z}}\left(\left(k_{pz}+\frac{k_{iz}}{s}\right)+\sum_{n=3,9}\frac{2\omega_c K_{qrn}}{s^2+2\omega_c s+(n\omega)^2}\right), \qquad (15)$$

where k_{pz} and k_{iz} are the parameters of ZSCC-PI controller, K_{qrn} is the nth harmonic resonant coefficient, ω_c is the QRC cut-off angular frequency, and n is the harmonic order that needed to be eliminated.

k_{pz} and k_{iz} are calculated using pole placement method as:

$$\begin{cases} k_{pz} = \dfrac{(L_{f1}+L_{f2})\zeta\omega_{nz}-(R_{f1}+R_{f2})}{V_{dc}} \\ k_{iz} = \dfrac{(L_{f1}+L_{f2})\omega_{nz}^2}{V_{dc}} \end{cases}, \qquad (16)$$

where ω_{nz} is the cut-off frequency of ZSCC PI controller.

The eq. (17) demonstrates that the QRC has two factors K_{qrn} and ω_c. In this case and for a good Bode diagram analysis, one of both factors must be fixed that makes easy to study and observe the impact of the other factor on the system performance.

Firstly, the factor K_{qrn} is kept equal to 1 and ω_c is varied; the Bode diagram of QRC in this case is shown in Fig. 6.

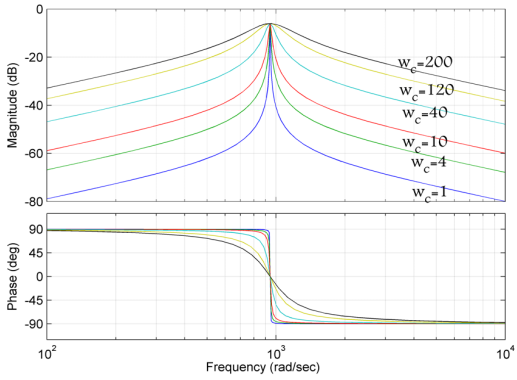

Fig. 6 – Bode diagram of QRC when ω_c is varied and K_{qr} is fixed

In second case, when ω_c is fixed to 1 rad/s and K_{qrn} is varied, the Bode diagram of QRC is shown in Fig. 7.

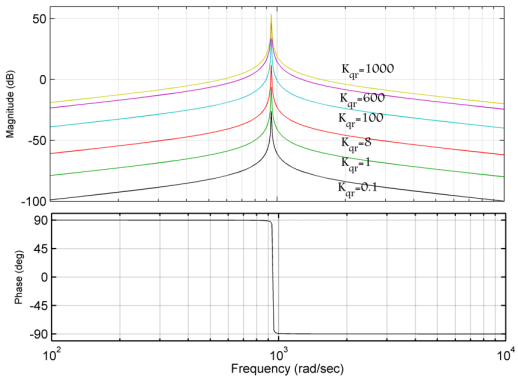

Fig. 7 – Bode diagram of QRC when K_{qr} is varied and ω_c is fixed

Figures 6 and 7 show that the band-pass filter gain is set to 0 dB at the 3rd harmonic frequency, and it can be also observed that the ω_c affects both QRC bandwidth and gain, and K_{qrn} affects only the gain of QRC. So, the increase of ω_c impacts the increase of QRC bandwidth and gain, and the increase of K_{qrn} impacts the increase of the gain. From this analysis, ω_c is selected depending on the QRC bandwidth and K_{qrn} is selected depending on the QRC gain.

On the basis that the ZSCC control is stable, one has just to increase sufficiently K_{qrn} to enhance the tracking of 3rd and 9th harmonics while also to resist all perturbations so that we can realize high-accuracy control of the ZSCC.

Based on the QRC Bode analysis and as described in [24], the parameters ω_c and K_{qrn} for 3rd and 9th harmonics are selected as follows: ω_c=5 rad/s, K_{qr3} =400 and K_{qr9} =200.

5. SIMULATION STUDY

To confirm the viability of the theoretical analysis and effectiveness of the proposed ZSCC-PIQRC method, simulation tests have been developed on the Matlab/Simulink using Sim Power Systems and S-Function. The simulation parameters of the two parallel PWM rectifier systems are presented in Table 1.

Table 1

System simulation parameters

Parameter	Value
Maximal voltage of ac grid V_{gmax}	120 V
Fundamental frequency of ac grid	50 Hz
Dc-bus voltage V_{dc}	300 V
Capacitor of dc side rectifiers C_{dc}	2 mF
Load resistance R_L	100 Ω
Ac-side filter inductance L_{f1}	10 mH
Ac-side filter inductance L_{f2}	6 mH
Ac-side resistances R_{f1} and R_{f2}	0.2 Ω
Switching frequency f_s	8 kHz

Figures 8 to 11 show the performance of two parallel PWM rectifiers with and without ZSCC control under both identical and unbalanced filters inductors. Two control methods are adopted herein to face ZSCC; the first one is based on traditional PI controller and the second is based on quasi resonant PI controller.

The all simulation waveforms from (a) to (f), respectively, are: a) first phase grid current and its corresponding voltage, b) DC-bus voltage, c) rectifiers' inputs currents i_{fa1} and i_{fa2}, d) ZSCC, e) spectrum analysis of i_{fa1}, and f) spectrum analysis of i_{fa2}.

Using all control methods, the two parallel PWM rectifiers system has similar performance regarding to the three-phase ac grid reactive power compensation and dc-bus voltage regulation (Figs. 8, 10 and 11 (a and b)).

In the case of identical inductances (Figs. 8), it can be observed that the input currents of the two PWM rectifiers i_{fa1} and i_{fa2} are sinusoidal and completely identical as shown in Fig. 8 (c). From Fig. 8(d), a small value of ZSCC (i_z) is generated in this case with very lower input currents THDs for the two PWM rectifiers as in Figs. 8 (e and f). The THD of i_{fa1} is 1.21 % and that of i_{fa2} is 1.20 %.

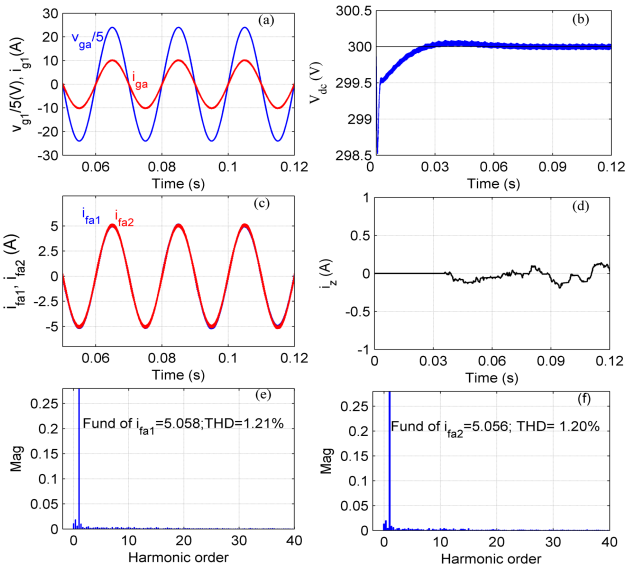

Fig. 8 – Simulations results with L_{f1}= L_{f2}=10 mH: a) first phase grid current and its corresponding voltage.

Figure 9 presents the behavior of the parallel system when L_{f1}= 10 mH and L_{f2}= 6 mH. It can be observed from Fig. 9 (d) that a very large ZSCC is generated. This ZSCC causes high distortion on the rectifiers' inputs currents as well as large magnitude values of 3rd and 9th harmonics as shown in the FFT analysis of these input currents as illustrated in Figs. 9 (e and f). The THD of i_{fa1} is increased from 1.21% in the case of identical inductances (Fig. 8 (e)) to 5.22 % in the case of unbalanced inductances (Fig. 9 (e)) and the THD of i_{fa2} is increased from 1.20 % (Fig. 8 (f)) to 5.19% (Fig. 9 (f)), which does not fit the IEEE Std 519 for current distortion limits. In this case, the inputs currents harmonics with high magnitude are mainly the 3rd and 9th.

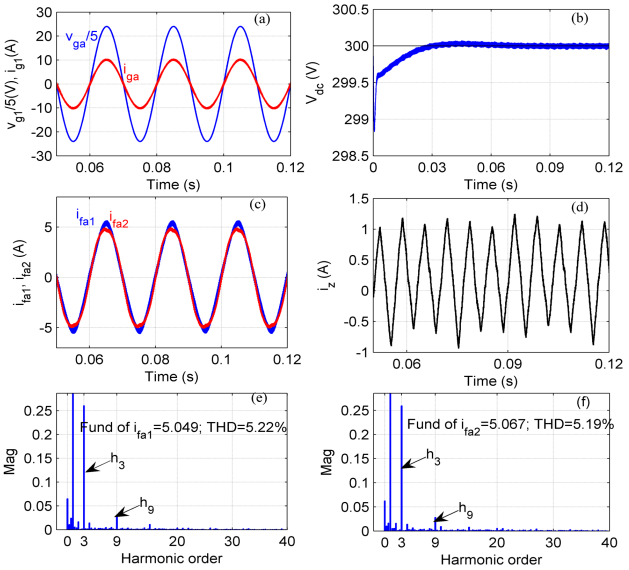

Fig. 9 – Simulations results with L_{f1}=10 mH and L_{f2}=6 mH without ZSCC control

By using ZSCC-PI control method, better ZSCC harmonics suppression and rectifiers' inputs currents harmonics elimination can be seen in Figs. 10(c, d, e and f).

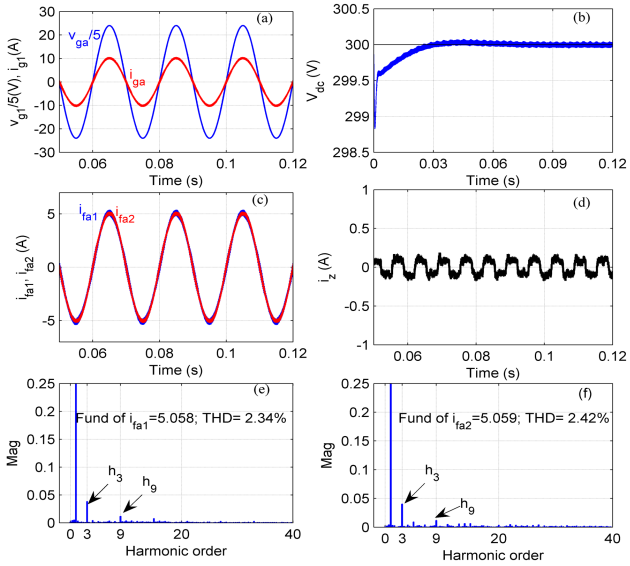

Fig. 10 – Simulations results with L_{f1}=10 mH and L_{f2}=6 mH, using the ZSCC-PI control

With the proposed method, as illustrated in Figs. 11, the ZSCC is almost totally suppressed (Fig. 11(e)). The ripples and the 3rd and 9th harmonics in the input currents of the two PWM rectifiers are further reduced significantly to very small values compared with ZSCC-PI. As can be seen from Figs. 11 (e and f), by using ZSCC-PI, the THDs of rectifier input currents i_{fa1} and i_{fa2} are 2.34 % and 2.42 %, respectively, which is in concordance with IEEE Std.

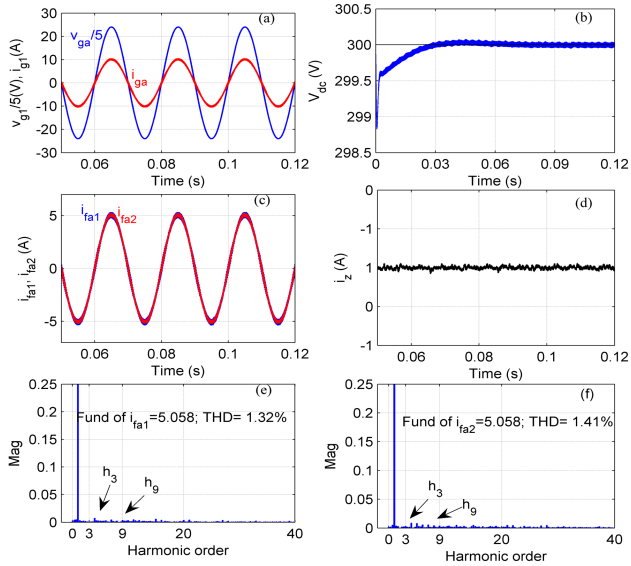

Fig. 11 – Simulations results with L_{f1}=10 mH and L_{f2}=6 mH, using the proposed PIQRC: a) first phase grid current and its corresponding voltage.

As shown in Figs. 11 (e and f), the rectifiers' inputs currents THD are further reduced to very small values (1.32 % and 1.41 %), and as expected, the rectifiers' input currents distortions are almost eliminated with very small 3rd and 9th harmonics and ripples.

To sum up, the proposed method can effectively eliminate the ZSCC and input currents harmonics especially the 3rd and 9th components with good performance. These results verify the viability of the theoretical analysis and the effectiveness of the proposed PIQRC for controlling the two parallel PWM rectifiers.

7. CONCLUSIONS

This paper proposes an ASVPWM strategy with a ZSCC control based on the quasi-resonant controller for two parallel three-phase PWM rectifiers to suppress the ZSCC and improve the power quality of the rectifiers' ac sides. An analysis of the ZSCC model and a detailed explanation of the proposed PIQRC method-based Bode diagram is provided. A comparative study with the conventional SVPWM and ASVPWM with ZSCC-PI confirms the validity and performance of the proposed method. The results of the parallel system with conventional SVPWM showed that a ZSCC appears when there are unequal filter inductances. As a result, the rectifiers' input currents are distorted with high magnitude, mainly the 3rd and 9th components, due to the ZSCCs influence. When the ZSCC-PI-based ASVPWM method is utilized, acceptable ZSCC suppression and rectifiers' inputs currents ripples. Harmonics elimination can be achieved, but when the proposed method is applied, the variable z can be accurately obtained at a periodic waveform of 150 Hz, resulting in high suppression of ZSCC and input currents ripples and harmonics, especially the 3rd and 9th components.

As a result, the proposed method can suppress the ZSCC and eliminate the input currents ripples and low-frequency harmonics, especially the 3rd and 9th components, and compensate for the reactive power in the grid.

Received on 24 April 2022

REFERENCES

1. J. Weidong, M. Weicheng, W. Jinping, W. Wei, Z. Xuewei, W. Lei, *Suppression of zero-sequence circulating current for parallel three-phase grid-connected converters using hybrid modulation strategy*, IEEE Trans. Ind. Electron., **65**, *4*, pp. 3017–3026 (2018).
2. A. Zorig, M. Belkheiri, S, Barkat, A. Rabhi, F. Blaabjerg, *Sliding mode control and modified SVM for suppressing circulating currents in parallel-connected inverters*, Electric Power Comp. and Syst., **46**, *9*, pp. 1061–1071 (2018).
3. A. Chebabhi, M.K. Fellah, M.F. Benkhoris, *Fuzzy logic and selectivity controllers for the paralleling of four-leg shunt active power filters based on three-dimensional space vector modulation*, IEEE, 3rd International Conference on Control, Engineering and Information Technology, Tlemcen, Algeria (25–27 May 2015).
4. X. Zhuang, L. Rui, X. Dianguo, *Control of parallel multi rectifiers for a direct drive permanent-magnet wind power generator*, IEEE Trans. Ind. Appl., **49**, *4*, pp. 1687–1696 (2013).
5. X.G. Zhang, W.W. Li, Y. Xiao, G.L. Wang, D.G. Xu, *Analysis and suppression of circulating current caused by carrier phase difference in parallel voltage source inverters with SVPWM*, IEEE Trans. Power Electron, **33**, *12*, pp. 11007–11020 (2018).
6. X. Zhang, J. Chen, Y. Ma, Y. Wang, D. Xu, *Bandwidth expansion method for circulating current control in parallel three-phase PWM converter connection system*, IEEE Trans. Power Electron., **29**, *12*, pp. 6847–6856 (2014).
7. Y. Peng, F. Han, *A Novel Lyapunov function-based nonlinear controller to suppress circulating current of paralleled multi-inverters*, IEEE International Conference on Computer Systems, Electronics, and Control (ICCSEC), Dalian, China, 25–27 Dec. 2017.
8. N. Jiahao, C. Ruirui, Z. Zheyu, G. Handong, W. Fred, M.T. Leon, J.B. Benjamin, J. C. Daniel, B. C. Benjamin, *Analysis of circulating harmonic currents in paralleled three level ANPC inverters using SVM*, IEEE Applied Power Electronics Conference and Exposition (APEC), Anaheim, CA, USA (17–21 March 2019).
9. M. Abbes, I. Mehouachi, S. Chebbi, *Circulating current reduction of a grid-connected parallel interleaved converter using energy shaping control*, Electric Power Systems Research, **170**, pp. 184–193 (2019).
10. F. Forest, E. Labouré, T.A. Meynard, V. Smet, *Design and comparison of inductors and intercell transformers for filtering of PWM inverter output*, IEEE Trans. Power Electron., **24**, pp. 812–821 (2009).
11. M. Ramkrishan, G. Ghanshyamsinh, B. Lorand, M. N. Stig, *Analysis and modelling of circulating current in two parallel-connected inverters*, IET. Power Electron., **8**, *7*, pp. 1273–1283 (2015).
12. X. Hanwei, X. Lie, L.W. Chi, Kui, Z. Zedong, L. Yongdong, *Improved interleaved discontinuous PWM for zero-zequence circulating current reduction in three-phase paralleled converters*, IEEE Trans. Ind. Electron. **68**, *9*, pp. 8676–8686 (2020).
13. K.K. Shafiuzzaman, B. Malabika, F.C. Michael, *Selection of design parameters to reduce the zero-sequence circulating current flow in parallel operation of dc linked multiple shunt APF units*, Adv. Power. Electron., 381581 (2013).
14. Z. Quan, Y. Li, *Suppressing zero-sequence circulating current of modular interleaved three-phase converters using carrier phase shift PWM*, IEEE Trans. Ind. Appl., **53**, *4*, pp. 3782–3792 (2017).
15. Z. Xueguang, F. Zhicao, X. Yi, W. Gaolin, X. Dianguo, *Control of parallel three-phase PWM converters under generalized unbalanced operating conditions*. IEEE Trans. Power Electron., **32**, *4*, pp. 3206–3215 (2017).
16. Z. Yijie, N. Heng, *Zero-sequence circulating current strategy of open-winding PMSG system with common dc bus based on zero vector redistribution*, IEEE Trans. Ind. Electron., **62**, *6*, pp. 3399–3408 (2015).
17. X. Zhang, W. Zhang, J. Chen, D. Xu, *Deadbeat control strategy of circulating currents in parallel connection system of three-phase PWM converter*, IEEE Trans. Energy Convers, **29**, *2*, pp. 406–417, (2014).
18. X. Zhang, T. Wang, X. Wang, G. Wang, Z. Chen, D. Xu, *A coordinate control strategy for circulating current suppression in multi paralleled three-phase inverters*, IEEE Trans. Ind. Electron., **64**, *1*, pp. 838–847 (2017).
19. Z. Zhiyong, L. Zhongxi, M. G. Stefan, *Space vector based hybrid PWM for zero-sequence circulating current RMS and common mode voltage reduction in two parallel interleaved two level converters*, J. Electric. Engin. Techn., **15**, pp. 1195–1204 (2020).
20. A. Chebabhi, M.K. Fellah, M.F. Benkhoris, *3D space vector modulation control of four-leg shunt active power filter using pq0 theory*, Rev. Roum. Sci. Techn. – Électrotechn. Et Énerg., **60**, *2*, pp. 371–376 (2015).
21. D. Beriber, A. Talha, A. Kouzou, A. Guichi, F. Bouchafaa, *multilevel inverter for grid-connected photovoltaic systems*, Rev. Roum. Sci. Techn. – Électrotechn. Et Énerg., **67**, *2*, pp. 105–110 (2022).
22. H. Serghine, R. Merahi, R. Chenni, D. Buła, *Combined operation of photovoltaic and active power filter system connected to nonlinear load*, Rev. Roum. Sci. Techn. – Électrotechn. Et Énerg., **64**, *4*, pp. 185–194 (2019).
23. S. Gulur, V. Mahadeva Iyer, S. Bhattacharya, *Proportional Integral - Resonant and Dual Loop Current Control Structure Comparison For Grid Connected Converters in the Rotating Frame*, IEEE Applied Power Electronics Conference and Exposition (APEC), San Antonio, TX, USA, 4–8 March 2018.
24. T. Song, P. Wang, Y. Zhang, F. Gao, Y. Tang, S. Pholboon, *suppression method of current harmonic for three-phase PWM rectifier in EV charging system*, IEEE Trans. on Vehic. Techn, **69**, *9*, pp. 9634–9642 (2020).